

PREPARED FOR SUBMISSION TO JINST

18TH INTERNATIONAL SYMPOSIUM ON LASER-AIDED PLASMA DIAGNOSTICS

24 - 28 SEPTEMBER 2017

PRAGUE, CZECH REPUBLIC

Estimation of reliable range of electron temperature measurements with sets of given optical bandpass filters for KSTAR Thomson scattering system based on synthetic Thomson data

Keon-hee Kim,^a Tae-suk Oh,^a Kyeo-reh Park,^a J.H. Lee,^b Y.-c. Ghim,^{a,1}

^a*Department of Nuclear and Quantum Engineering, KAIST, Daejeon, Korea*

^b*National Fusion Research Institute, Daejeon, Korea*

E-mail: ycghim@kaist.ac.kr

ABSTRACT: One factor determining the reliability of measurements of electron temperature using a Thomson scattering (TS) system is transmittance of the optical bandpass filters in polychromators. We investigate the system performance as a function of electron temperature to determine reliable range of measurements for a given set of the optical bandpass filters. We show that such a reliability, i.e., both bias and random errors, can be obtained by building a forward model of the KSTAR TS system to generate synthetic TS data with the prescribed electron temperature and density profiles. The prescribed profiles are compared with the estimated ones to quantify both bias and random errors.

KEYWORDS: Plasma diagnostics - interferometry, spectroscopy and imaging; Analysis and statistical methods; Data processing methods

¹Corresponding author.

Contents

1	Introduction	1
2	Forward model of the KSTAR Thomson scattering system	2
3	Comparison between the prescribed T_e and the estimated T_e	5
4	Conclusion	7

1 Introduction

Thomson scattering (TS) diagnostic system is widely used to measure both temperature and density of electrons in hot fusion-grade plasmas. Broadening of the spectral distribution of the Thomson scattered light is a function of electron temperature; whereas the intensity of the light contains the information of electron density [1]. The KSTAR TS system collects the scattered light with polychromators consisting of a set of five optical bandpass filters [2] as shown in figure 1. Reliably measurable ranges of temperature depend on the properties of the filters such as central wavelength, bandwidth and the number of the filters.

Achievable fractional errors given a set of the filters together with TS system parameters have been estimated by considering measured signal level of background and scattered light with an electronic, i.e., amplifiers, noise [3–5]. Such fractional errors provide quantitative magnitude of random errors but do not present bias errors. With the aim of obtaining both bias (if finite) and random errors, we have developed a forward model of the KSTAR TS system and generated

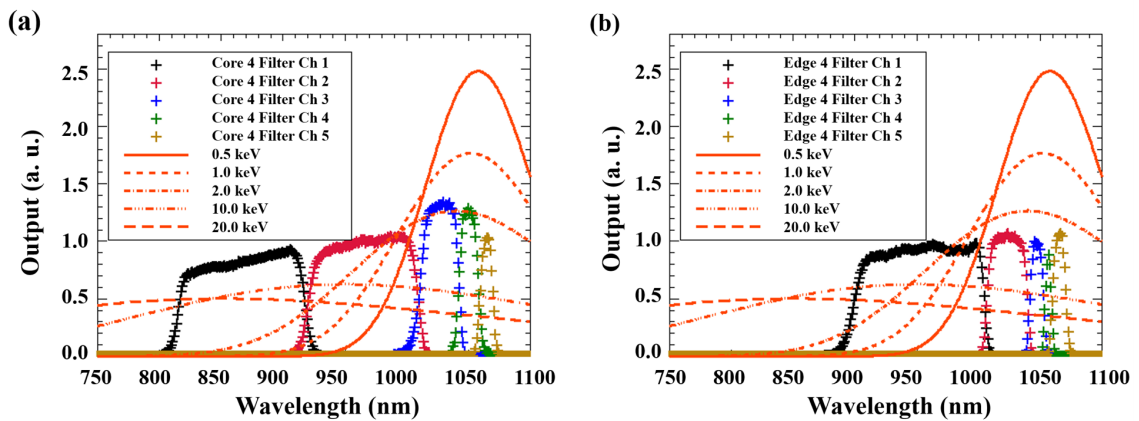


Figure 1. Examples of measured transmittance of the optical bandpass filters (+) with spectral distributions of Thomson scattered lights for various electron temperatures (lines) for (a) Core #4 and (b) Edge #4 of the KSTAR TS polychromators used during the 2016 Campaign.

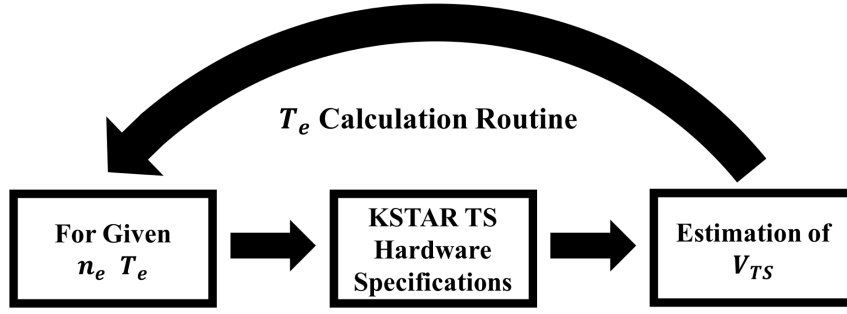


Figure 2. A schematic of the KSTAR TS forward model. Expected (synthetic) TS data are generated based on the KSTAR TS system specifications, and the synthetic data are analyzed as if they were actual experimental data. Then, results are compared with the prescribed profiles of electron density and temperature to estimate the reliability of the KSTAR TS system.

synthetic TS data [6] with prescribed profiles of electron density and temperature. The forward model is based on the TS system parameters used during the 2016 KSTAR campaign.

Treating the synthetic TS data as if they were experimentally measured ones, we can obtain temperature and density of electrons by using a look-up table method [6, 7] which, then, are compared with the prescribed temperature and density. Figure 2 schematically describes such a procedure. This will allow us to quantify both bias and random errors. In this paper, we investigate the reliability of estimating various profiles of electron temperature with a fixed density profile.

2 Forward model of the KSTAR Thomson scattering system

Laser pulse with the wavelength of 1064 nm is tangentially injected from the L-port of KSTAR [8] and the Thomson scattered photons are collected via edge and core optical systems as shown in figure 3. These photons are passed to polychromators, where each polychromator contains five optical bandpass filters. Combinations of central wavelengths and bandwidths are different between core and edge polychromators as shown in figure 1(a) and (b), respectively. Photons passed through a bandpass filter are detected by an avalanche photodiode detector (APD: Hamamatsu S11519-30). Since there are five bandpass filters in a polychromator, we have five APDs for each polychromator.

Each APD outputs an electronic signal proportional to the detected photons, and this signal can be modelled as [3, 6],

$$V_{TS}^i = G n_e N_{laser} \frac{d\sigma_{TS}}{d\Omega} \Delta\Omega L T(\lambda_L) QE \int \frac{\phi^i(\lambda_s) S(\lambda_s; T_e, \theta, \lambda_L)}{\phi(\lambda_L) \lambda_L} d\lambda_s, \quad (2.1)$$

where superscript i denotes the i^{th} channel of the optical bandpass filters in a given polychromator. G , n_e , N_{laser} and $\frac{d\sigma_{TS}}{d\Omega}$ correspond to the APD gain factor, the electron density, the number of injected photons in a single laser pulse and the differential Thomson scattering cross-section, respectively. $\Delta\Omega$ and L are the solid angle and the scattering length of the KSTAR TS system, respectively. Transmission coefficient is a function of wavelength, and this is captured via taking the absolute coefficient at the laser wavelength $T(\lambda_L)$ ($\lambda_L = 1064$ nm is the laser wavelength) with the normalized filter transmittance function (or just simply filter function) $\phi^i(\lambda_s)/\phi(\lambda_L)$, where λ_s is the scattered

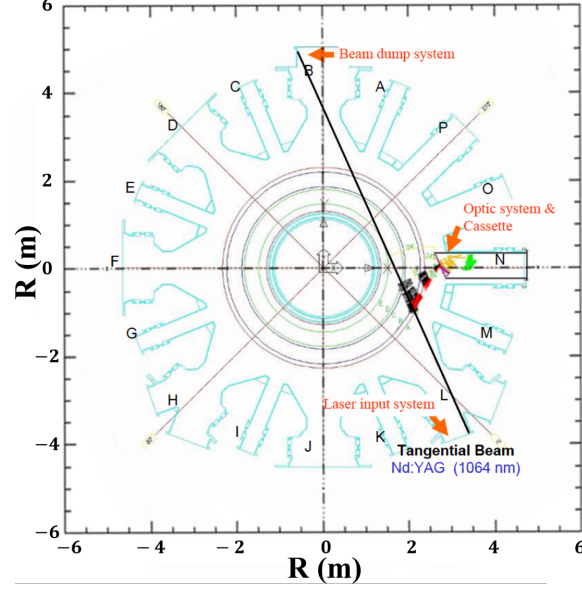


Figure 3. Top view of the KSTAR TS system. Nd:YAG laser pulse with the wavelength of 1064 nm is injected tangentially from the L-port, and the laser beam dump is located at the B-port. Thomson scattered light is collected via edge (red dashed lines) and core (black dashed lines) optical systems at the N-port.

wavelength. Figure 1(a) and (b) show such normalized filter functions (+). Note that the quantum efficiency QE of the APD detector is also a function of the wavelength, but such a variation is captured by the filter function $\phi^i(\lambda_s)$ as well; thus QE in equation (2.1) is the quantum efficiency at the laser wavelength. $S(\lambda_s; T_e, \theta, \lambda_L)$ is a spectral distribution of the Thomson scattered light [1, 9] as a function of the scattered wavelength λ_s at a certain electron temperature T_e , scattering angle θ and laser wavelength λ_L .

To be able to generate expected (or synthetic) KSTAR TS data based on equation (2.1), we need to use hardware specifications of the KSTAR TS system which are listed in table 1. The KSTAR TS system measures electron density and temperature at 12 spatial positions with the core optical system, i.e., $R = 1.81, 1.84, 1.87, 1.90, 1.96, 1.98, 2.02, 2.05, 2.08, 2.10, 2.13$ and 2.16 m, and 15 spatial positions with the edge optical system, i.e., $R = 2.16, 2.17, 2.18, 2.19, 2.20, 2.21, 2.22, 2.23, 2.24, 2.25, 2.26, 2.27, 2.28, 2.29$ and 2.30 m, where R is the major radius. Note that a typical location of the magnetic axis in KSTAR is $R_0 \approx 1.80$ m. Depending on the spatial positions, scattering angle θ and scattering length L are different, and they have been calculated based on the

Table 1. Specification of the KSTAR TS system used during the 2016 Campaign.

	Core Optical System	Edge Optical System
Laser Energy	2 J	2 J
F/#	5.6	6.5
Solid Angle ($\Delta\Omega$)	0.0250	0.0186
Transmission Coefficient at λ_L (T)	0.57	0.57
Quantum Efficiency λ_L (QE)	0.58	0.58

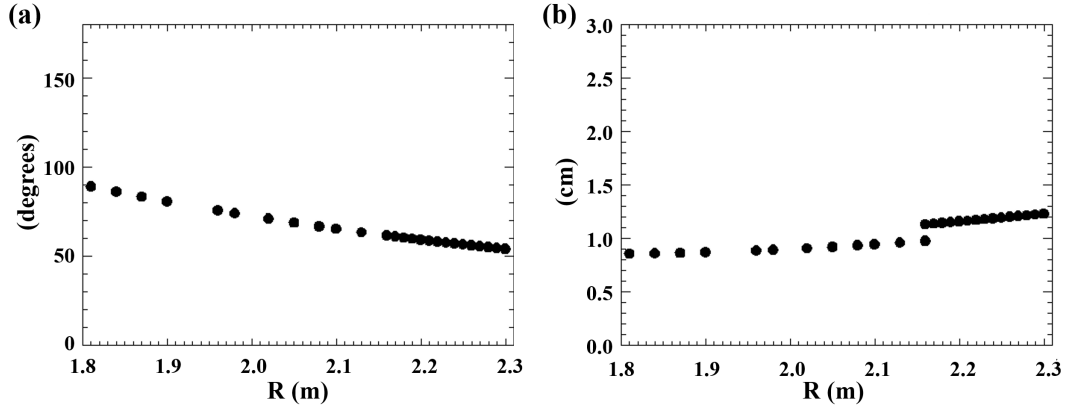


Figure 4. Calculated (a) scattering angle θ and (b) scattering length L as a function of the major radius R for the KSTAR TS system used during the 2016 Campaign.

geometry of the KSTAR TS system (e.g. figure 3). Scattering angle and length as a function of the major radius R are shown in figure 4.

Collected number of scattered photons as a function of the scattered wavelength denoted as n_s just before passing a polychromator can be written as

$$n_s(\lambda_s) = n_e N_{\text{laser}} \frac{d\sigma_{\text{TS}}}{d\Omega} \Delta\Omega L T(\lambda_L) \frac{S(\lambda_s; T_e, \theta, \lambda_L)}{\lambda_L}, \quad (2.2)$$

and the number of photo-electrons N_s from an APD detector can be written as

$$N_s(\lambda_s) = n_s(\lambda_s) QE \frac{\phi^i(\lambda_s)}{\phi(\lambda_L)}. \quad (2.3)$$

Figures 5 and 6 show examples of collected scattered photons $n_s(\lambda_s)$ and photo-electrons $N_s(\lambda_s)$ detected by the Core #4 polychromator ($R = 1.90$ m) when $T_e = 1.9$ keV and $n_e = 1.0 \times 10^{19} \text{ m}^{-3}$.

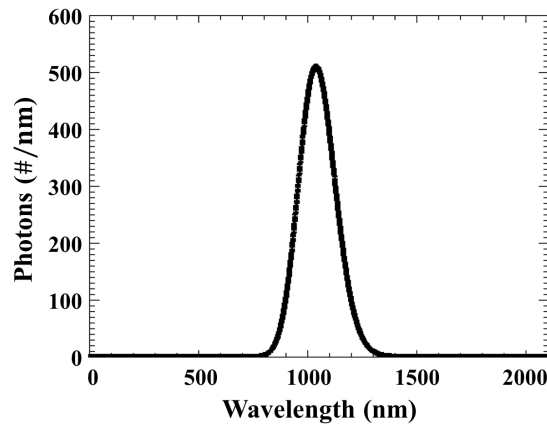


Figure 5. Spectral distribution of collected scattered photons $n_s(\lambda_s)$ for Core #4 ($R = 1.90$ m) when $T_e = 1.9$ keV and $n_e = 1.0 \times 10^{19} \text{ m}^{-3}$.

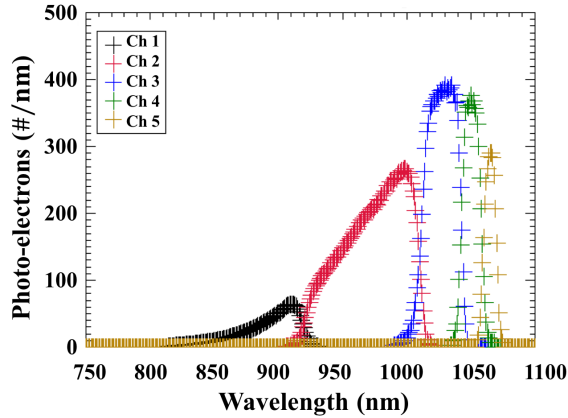


Figure 6. Spectral distribution of photo-electrons $N_s(\lambda_s)$ detected by five APD detectors of the Core #4 polychromator ($R = 1.90$ m) when $T_e = 1.9$ keV and $n_e = 1.0 \times 10^{19} \text{ m}^{-3}$.

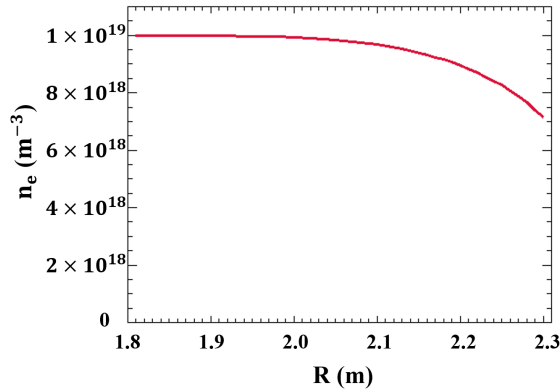


Figure 7. A typical electron density profile of L-mode discharge observed in KSTAR.

Integrating photo-electrons with respect to the scattered wavelength λ_s and multiplying it with the APD gain factor G provides the electronic signal that we can read using a digitizer, i.e., equation (2.1). For the purpose of this paper, actual value of G is irrelevant because the KSTAR TS system is dominated by the photon noise [6] which means that noise levels are determined by the number of photo-electrons. We note that our forward model can act as a likelihood function in the frame of Bayesian probability theory [10].

3 Comparison between the prescribed T_e and the estimated T_e

Based on the KSTAR TS forward model described in section 2, we generate the KSTAR TS synthetic data with a typical electron density profile of L-mode discharge observed in KSTAR as shown in figure 7, while varying profiles of electron temperature. Depending on the total number of photo-electrons from an APD detector (e.g. figure 6), we add random Poisson noise to the signal. Using a look-up table method [6, 7], we estimate electron temperature from the noise added synthetic data. Although the KSTAR TS system contains five bandpass filters and five APD

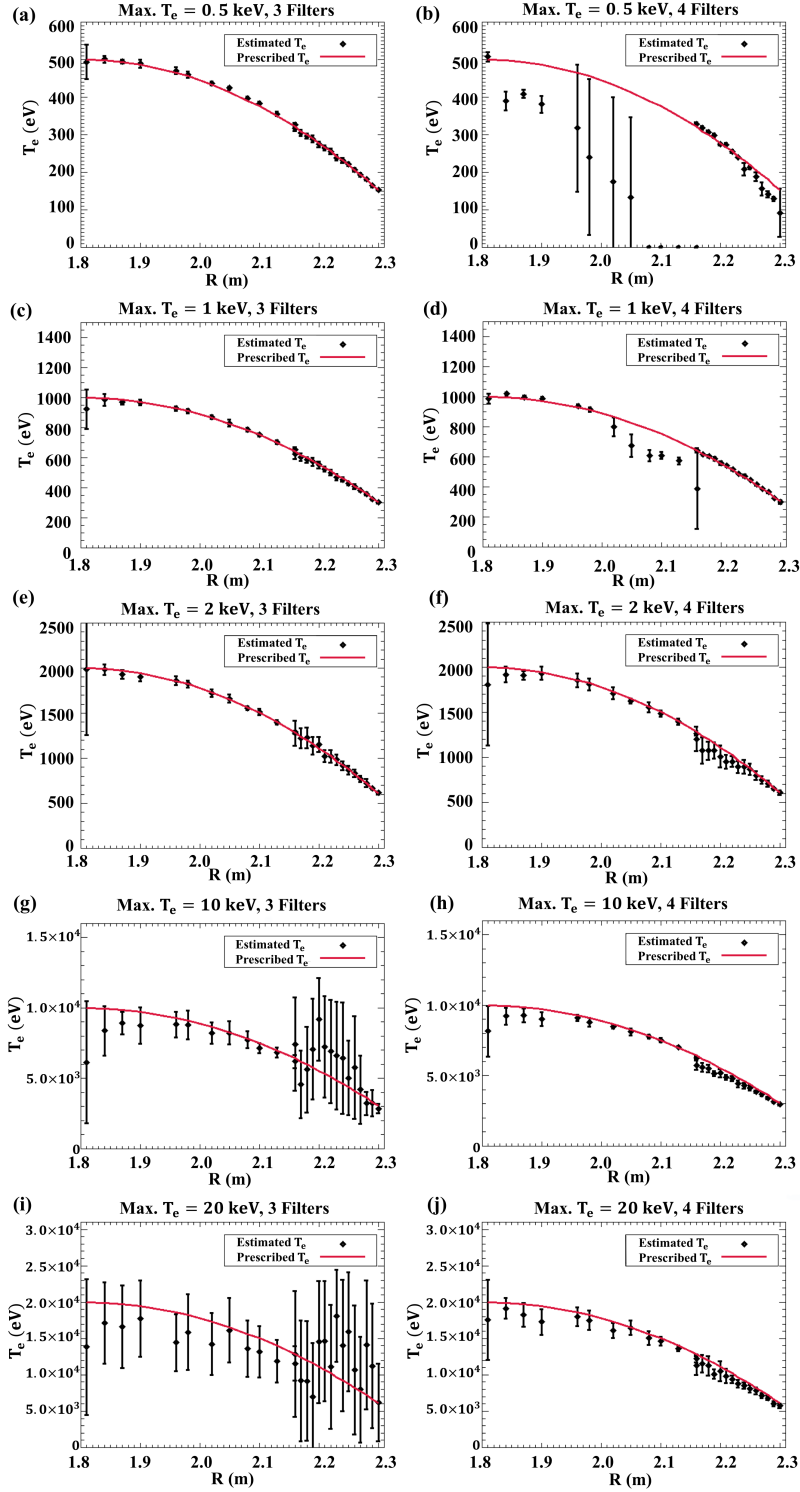


Figure 8. Comparison between the prescribed (red line) and estimated (dots) electron temperature T_e based on the KSTAR TS synthetic data. Ten data sets are used to estimate a profile of T_e for each prescribed T_e profile. Means are marked with dots, whereas error bars represent standard deviations.

detectors denoted as Ch.1 to Ch.5 for each polychromator, Ch.5 is excluded from the temperature estimation because Ch.5 is strongly affected by the stray light [6] as the laser wavelength, i.e., 1064 nm, is within the bandpass of this channel (see figure 1). In using the look-up table method, we have examined two cases: 1) using three filters (or channels), i.e., Ch.2, Ch.3 and Ch.4, and 2) using four filters (or channels), i.e., Ch.1, Ch.2, Ch.3 and Ch.4. We generate ten data sets from which mean and random error (standard deviation) are estimated for a given temperature profile where the randomness is added by the Poisson noise. Comparisons between the prescribed and estimated electron temperatures for these two cases with various electron temperatures are shown in figure 8. Note that the polychromator observing the most inner location, i.e., $R = 1.81$ m uses ‘edge’ bandpass filters even if it is defined as ‘core’ polychromators.

For the core polychromator system whose combination of bandpass filters is shown in figure 1(a), we find that using four filters (Ch.1 to Ch.4) for estimating $T_e < 0.8$ keV results in underestimation, i.e., bias error, and relatively larger uncertainties compared to using three filters (Ch.2 to Ch.4) from figure 8(a)-(d). Since the bandpass of Ch.1 is farthest away from the laser wavelength, relatively low temperature generates very small amount of photo-electrons for Ch.1 resulting in a very small signal-to-noise ratio. On the other hand, using four channels gives us better temperature estimation for $T_e > 10$ keV as in figure 8(g)-(j). For such a large temperature, we now have a good signal-to-noise ratio for Ch.1, and this channel starts to provide additional valuable information for estimating temperature.

For the edge polychromator system shown in figure 1(b), we find that as long as $T_e < 5$ keV, either using three filters or four filters provides us reasonably good estimation of temperatures. If $T_e > 5$ keV, then using three filters results in the overestimation and larger uncertainties for estimating temperature compared to using four channels as in figure 8(g)-(j).

4 Conclusion

We have developed a forward model of the KSTAR TS system for the purpose of quantifying both bias and random errors in estimating electron temperature, where previous estimation of fractional errors provide just random errors. Our model can be used not only for the KSTAR TS system but also any other TS systems as the forward model is generic. For the examined KSTAR TS system, we find that three filters are to be used for core polychromators when electron temperature is less than 0.8 keV, while using four filters are recommended when the temperature is larger than 10 keV. For the edge polychromators, choice of using three or four filters is irrelevant as long as the temperature is less than 5 keV, and using four filters is recommended for the temperature greater than 5 keV.

Acknowledgments

This work is supported by National R&D Program through the National Research Foundation of Korea (NRF) funded by the Ministry of Science and ICT (grant numbers NRF-2017M1A7A1A01015892 and NRF-2017R1C1B2006248) and the KUSTAR-KAIST Institute, KAIST, Korea.

References

- [1] O. Naito, H. Yoshida and T. Matoba, *Analytic formula for fully relativistic Thomson scattering spectrum*, *Phys. Fluids B*, **5** (1993) 4256.
- [2] J. H. Lee, S. T. Oh and H. M. Wi, *Development of KSTAR Thomson scattering system*, *Rev. Sci. Instrum.*, **81** (2010) 10D528.
- [3] R. Scannell, *Investigation of H-mode edge profile behaviour on MAST using Thomson scattering*, PhD thesis, University College Cork, 2007
- [4] R. Scannell et al., *Design of a new Nd:YAG Thomson scattering system for MAST*, *Rev. Sci. Instrum.*, **79** (2008) 10E730
- [5] H. G. Lee, J. H. Lee, D. Johnson, R. Ellis, R. Feder and H. Park, *Design of core and edge Thomson scattering systems for Korea Superconducting Tokamak Advanced Research tokamak*, *Rev. Sci. Instrum.*, **75** (2004) 3903.
- [6] T.-S. Oh, K. H. Kim, J. H. Lee, S. H. Lee, R. Scannell, A. R. Field, K. Cho, M. S. Bawa'aneh and Y.-c. Ghim, *Quantifying noise sources in the KSTAR 2014 Thomson scattering system from the measured variation on electron temperature*, *J. Instrum.*, **11** (2016) C03036.
- [7] S. Oh, J. H. Lee and H. M. Wi, *Examinations of electron temperature calculation methods in Thomson scattering diagnostics*, *Rev. Sci. Instrum.*, **83** (2012) 10D525.
- [8] J. H. Lee et al., *Tangential Thomson scattering diagnostic for the KSTAR tokamak*, *J. Instrum.*, **7** (2012) C02026.
- [9] S. L. Prunty, *A primer on the theory of Thomson scattering for high-temperature fusion plasmas*, *Phys. Scr.*, **89** (2014) 128001.
- [10] D. Sivia, *Data Analysis: a Bayesian Tutorial*, Oxford:Clarendon (1996)